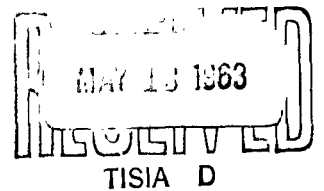


63-1

I  
I  
I  
-  
I  
I  
I  
I  
I  
I  
-  
I  
I  
I  
I  
I  
I  
I  
I  
I



QUARTERLY REPORT NO. 3  
for  
GALLIUM ARSENIDE VARACTOR DIODES  
THIS REPORT COVERS THE PERIOD  
28 DECEMBER 1962 TO 28 MARCH 1963  
RADIO CORPORATION OF AMERICA  
Semiconductor and Materials Division  
Somerville, New Jersey  
NAVY BUREAU OF SHIPS ELECTRONICS DIVISION  
CONTRACT NO. NOBSR 87405  
PROJECT SERIAL NO. SR-008031  
TASK NO. 9349 30 April 1963

Written By:

Henry Kressel  
H. Kressel

G.A. Kupsky  
G.A. Kupsky

Edited By:

L.R. Possemato  
L.R. Possemato

Approved By:

A. Blicher  
A. Blicher, Manager  
Special Projects  
Development

D.J. Donahue  
D.J. Donahue, Manager  
Industrial Transistor  
Development

DISTRIBUTION LIST

<u>Addressee</u>	<u>Copies</u>
Department of the Navy Bureau of Ships Semiconductor Group, Code 681A1A Washington 25, D.C. ATTN: Mr. A.H. Young	3
Department of the Navy Bureau of Ships, Code 335 Washington 25, D.C.	2
Department of the Navy Bureau of Naval Weapons, Code RREN-4 Washington 25, D.C.	1
Department of the Navy Bureau of Naval Weapons, Code RAAV-333 Washington 25, D.C.	1
Department of the Navy Office of Naval Research Chief of Naval Research, Code 427 Washington 25, D.C. ATTN: A.A. Shostak	1
Director U.S. Naval Research Laboratory Washington 25, D.C. ATTN: Code 2020	1
Director U.S. Naval Research Laboratory Washington 25, D.C. ATTN: A. Brodzinsky, Code 5210	1
Director U.S. Naval Research Laboratory Washington 25, D.C. ATTN: G. Abraham, Code 5266	1
Commander New York Naval Shipyard Material Laboratory, Code 923 Naval Base Brooklyn 1, New York	1
Commander U.S. Naval Ordnance Laboratory White Oak, Maryland ATTN: W.W. Scanlon	1

# DISTRIBUTION LIST (Cont.)

<u>Addressee</u>	<u>Copies</u>
Commanding Officer U.S. Army Signal Research and Development Laboratory Solid State Division ATTN: SIGRA/SL-PF (H. Jacobs)	1
Commander Aeronautical Systems Division ATTN: R.D. Alberts ASRNEM, AFSC Wright-Patterson Air Force Base Dayton, Ohio	1
Commander, ESD (AFCRL) ATTN: R.P. Dolan, CRR-CSA L.G. Hanscom Field Bedford, Massachusetts	1
Ordnance Corps, Department of the Army Diamond Ordnance and Fuze Laboratories Connecticut Avenue & Van Ness Street, N.W. Washington 25, D.C. ATTN: T.M. Liimatainen	1
Director National Bureau of Standards Electronics and Electricity Division Electronic Engineering Section Washington 25, D.C. ATTN: Gustave Shapiro	1
Advisory Group on Electron Devices 346 Broadway, 8th. Floor New York 13, New York ATTN: H.J. Sullivan	3
Commander Armed Services Technical Information Agency ATTN: TIAI Arlington Hall Station Arlington 12, Virginia	10
Armour Research Foundation Technology Center Chicago 16, Illinois ATTN: J.W. Buttrey	1
Batelle Memorial Institute 505 King Avenue Columbus, Ohio ATTN: C.S. Pett	1

DISTRIBUTION LIST (Cont.)

<u>Addressee</u>	<u>Copies</u>
Bell Telephone Laboratories Murray Hill, New Jersey ATTN: R.M. Ryder	1
Hughes Products Semiconductor Division 500 Superior Avenue Newport Beach, California ATTN: E.L. Steele	1
IBM Components Laboratory Bldg. 701 - Dept. 677 Poughkeepsie, New York ATTN: J.E. Thomas, Jr.	1
Massachusetts Institute of Technology Lincoln Laboratory Lexington 73, Massachusetts ATTN: R.H. Rediker	1
Philco Corporation Lansdale Division Lansdale, Pa. ATTN: C.G. Thornton	1
Raytheon Company Research Division Library 28 Seyon Street Waltham 54, Massachusetts	1
Sylvania Electric Products, Inc. Semiconductor Division 100 Sytan Road Woburn, Massachusetts ATTN: Research and Engineering Librarian	1
Texas Instruments, Inc. Central Research and Engineering P.O. Box 5474 Dallas 22, Texas ATTN: Technical Reports Service	1
General Electric Company Semiconductor Products Department Electronics Park, Syracuse, New York ATTN: N. Holonyak	1

DISTRIBUTION LIST (Cont.)

<u>Addressee</u>	<u>Copies</u>
Microwave Associates, Inc. Burlington, Massachusetts ATTN: A. Uhlir, Jr.	1
Micro State Electronics Corporation 152 Floral Avenue Murray Hill, New Jersey ATTN: A. Kestenbaum	1
Microwave Semiconductor and Instruments, Inc. 116-06 Myrtle Avenue Richmond Hill 18, New York ATTN: A. Lederman	1
Stanford Research Institute Material Sciences Division Menlo Park, California ATTN: F.A. Halden	1
American Electronic Laboratories, Inc. Richardson Road Colmar, Pa.	1
Tyco Laboratories, Inc. Bear Hill Waltham 54, Massachusetts	1

## TABLE OF CONTENTS

### PART I

	<u>Page</u>
I. PURPOSE . . . . .	1
II. TECHNICAL DISCUSSION . . . . .	2
A. Device Specification . . . . .	2
B. Process Development . . . . .	4
1. General . . . . .	4
2. Effects of Heat Treatment on Crystal Properties	6
3. Ohmic Contacts . . . . .	8
4. Epitaxial Diodes . . . . .	12
C. Final Results for Phase II . . . . .	18
III. CONCLUSIONS . . . . .	19

### PART II

I. PROGRAM FOR NEXT PERIOD . . . . .	20
--------------------------------------	----

# LIST OF FIGURES

<u>Figure No.</u>	<u>Title</u>	<u>Page</u>
1	Breakdown Voltage vs. Minimum Capacitance For 250 MW Diode Input Power at 12 GC (Best Conversion Efficiency) . . . . .	3
2	Well Structure Cross Section . . . . .	5
3	Junction Depth $X_j$ , As A Function of Diffusion Time For Zinc Into N-Type GaAs ( $n \approx 4 \times 10^{16}$ Donors/cc) . . . . .	7
4	Normalized Net Carrier Concentration Change vs. Starting Concentrations After 3 Min. At 1000°C for Several N-Type GaAs Crystals . . . . .	9
5	Electron Mobility Before and After Heat Treatment (3 Min. at 1000°C) For Six N-Type GaAs Samples . . . . .	10
6	Normalized Resistivity Change $\frac{\rho}{\rho_0}$ , vs. Starting Resistivity, $\rho_0$ , For Several N-Type GaAs Crystals Diffused For 3 Minutes at 1000°C . . . . .	11
7	Contact Resistance Determination . . . . .	13
8	Breakdown Voltage As A Function of Impurity Gradient For PN GaAs Junctions . . . . .	16

# LIST OF TABLES

<u>Table No.</u>	<u>Title</u>	<u>Page</u>
I	Characteristic of Grown $P^+ NN^+$ Diodes . . . . .	15
II	Data For Varactor Diode - Device B . . . . .	17



ABSTRACT

Emphasis this quarter was placed on the fabrication of diodes with breakdown voltages in excess of 20 volts. Devices were made using both epitaxial and melt-grown material. The change in material characteristics which occur during diffusion have been investigated. Ten devices meeting the requirements outlined for Phase II of this contract have been delivered.

## PART I

### I. PURPOSE

The purpose of this contract is to develop a series of gallium arsenide varactor diodes capable of yielding 40% power conversion efficiency from 12 Gc to 24 Gc.

Phase II of this contract is to develop a device that is capable of meeting the following circuit objectives:

- (a) Input frequency of 12 Gc
- (b) Output frequency of 24 Gc
- (c) Input power of 100 mw
- (d) Output power equal to or greater than 40 mw at 25°C

This phase was completed on 2/28/63 with the delivery of 10 samples.

The goal of Phase III of the contract is to develop a device meeting the following objectives:

- (a) Input frequency of 12 Gc
- (b) Output frequency of 24 Gc
- (c) Input power of 250 mw
- (d) Output power of 100 mw minimum at 25°C

A total of ten units will be submitted to the contracting agency together with all the required reports.

## II. TECHNICAL DISCUSSION

### A. Device Specification

In the first quarterly report of this contract, expressions were derived for the power handling capability and conversion efficiency of a varactor diode. The maximum power input for optimum efficiency was shown to be:

$$P_{in} = \frac{1}{35} \omega C_{min} (\phi + V_B)^2 \dots \dots \dots (1)$$

where:

$\omega$  = input angular frequency

$C_{min}$  = minimum junction capacitance

$V_B$  = breakdown voltage

$\phi$  = built-in potential (1 volt for Gallium Arsenide)

Figure (1) shows the relationship between  $V_B$  and  $C_{min}$  which must be satisfied at 12 Gc for an input power level of 250 mw in order to obtain optimum conversion efficiency.

The conversion efficiency was shown to be determined by the ratio

$$\frac{f_{in}}{f_{c(max)}}$$

where:

$$f_{in} = \text{input frequency, } f_{c(max)} = \frac{1}{2\pi R C_{min}}$$

$R$  = diode series resistance

To obtain 40% conversion efficiency,  $\frac{f_{in}}{f_{c(max)}}$  must be equal to or

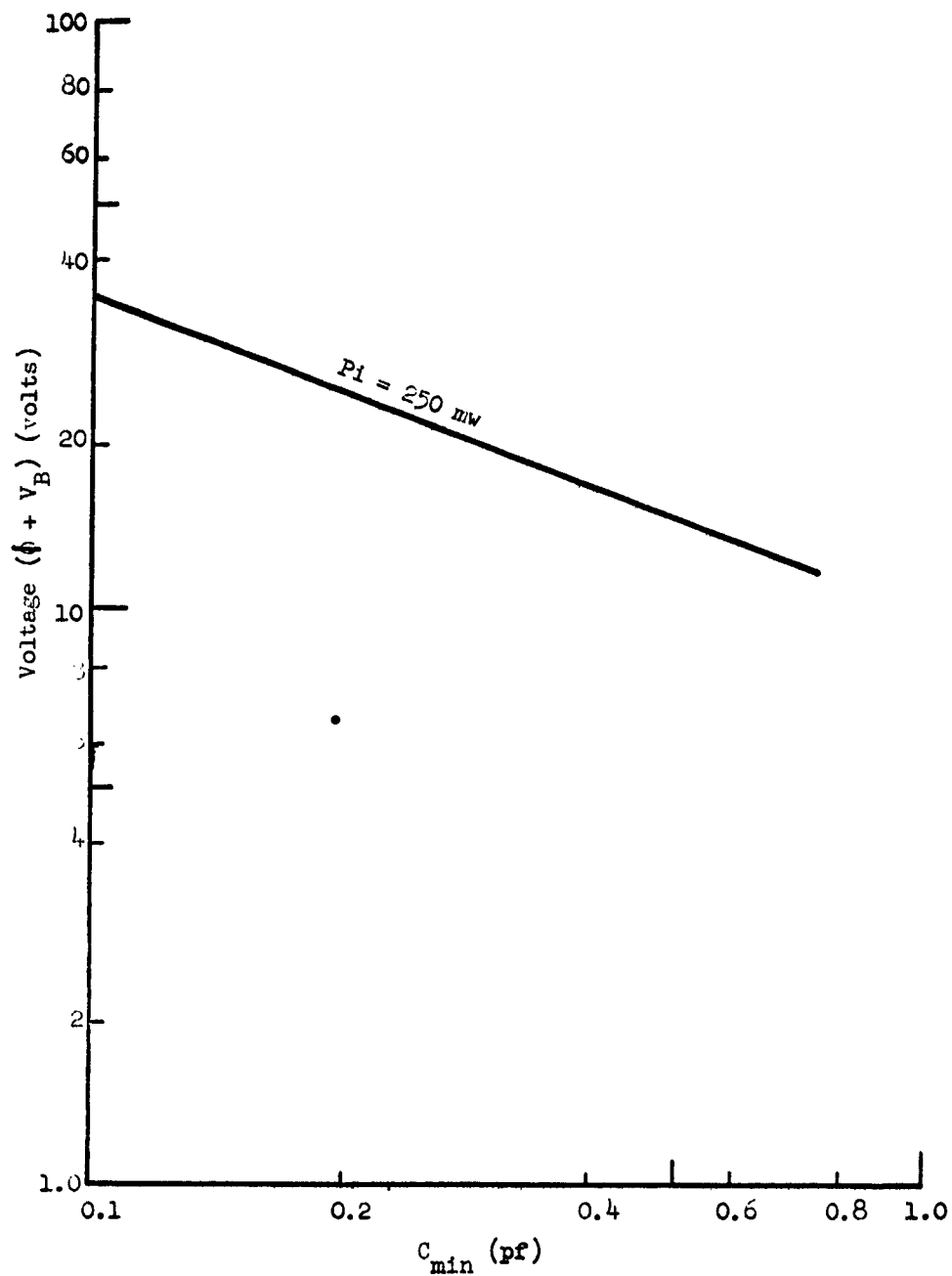


FIGURE 1 BREAKDOWN VOLTAGE vs. MINIMUM CAPACITANCE FOR 250 mW  
DIODE INPUT POWER AT 12 GC (BEST CONVERSION EFFICIENCY)

less than 0.050. At 12 Gc input frequency,  $f_{c(max)}$  must therefore, be greater than 240 Gc.

B. Process Development

1. General

The second quarterly report outlined the "well" process which was developed to minimize the series resistance of the devices. The well structure consists of a thin base region surrounded by thicker bulk material (Figure 2). Work continued during this quarter on improving the reproducibility of this technique. Two areas in particular have received a great deal of attention: parallel lapping of the wafers; and control of diffusion depth.

Since the wells are etched simultaneously over a whole wafer, the parallel tolerance of the wafer planes is obviously very important. Best results have been obtained by hand lapping, using a lapping fixture which give tolerances to within 0.05 mils. The final wafer thickness is approximately 3 mils.

Close control of the base region when the wells are etched prior to the p-type diffusion also requires close control of the diffusion depth. At the diffusion temperature previously used (1000°C), the diffusion coefficient for zinc in gallium arsenide is such that the typical diffusion run time was approximately 120 seconds for 0.4 mil penetration. Furthermore, the time required to bring the ampoule up to temperature was a very appreciable part of the total time in the furnace. Several experiments have been made with the temperature of diffusion reduced to 800°C which have resulted in substantially improving

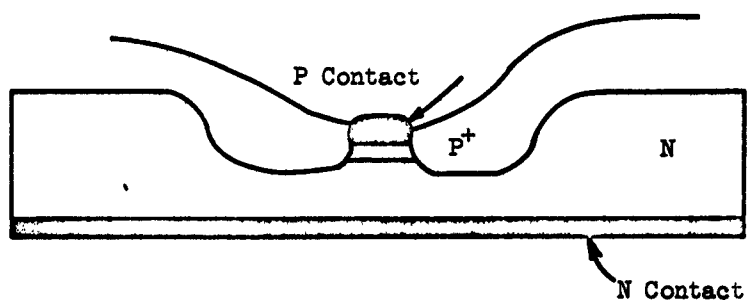


FIGURE 2 WELL STRUCTURE CROSS SECTION

the control of diffusion depth.

Figure 3 is a plot of junction depth  $X_j$ , as a function of time for three diffusion runs. The zinc surface concentration is about  $5 \times 10^{19}$  atoms/cc. The variation of  $X_j$  as a function of time follows from the normal erfc distribution:

$$X_j \propto \sqrt{t}$$

The calculated diffusion coefficient is equal to about  $2 \times 10^{-11}$  cm<sup>2</sup>/sec.

## 2. Effects of Heat Treatment on Crystal Properties

Since the fabrication of relatively high breakdown diodes (greater than 30-40 volts) requires relatively lightly doped starting material, the changes in the property of such crystal during diffusion are of great interest.

It has been observed that, in general, the measured values of cutoff frequency of the diodes fabricated from material with net carrier concentration under  $2 \times 10^{16}$ /cc are substantially below the expected values, if the spreading resistance is computed using the initial crystal resistivity. This discrepancy may be attributed in large part to the reduction in the net carrier concentration which is known to occur during high temperature heat treatment of n-type gallium arsenide. These changes are attributed to the introduction of contaminants during heat treatment which act as p-type impurities.

The degree of compensation has been measured on a number of n-type crystals with starting net carrier concentrations between

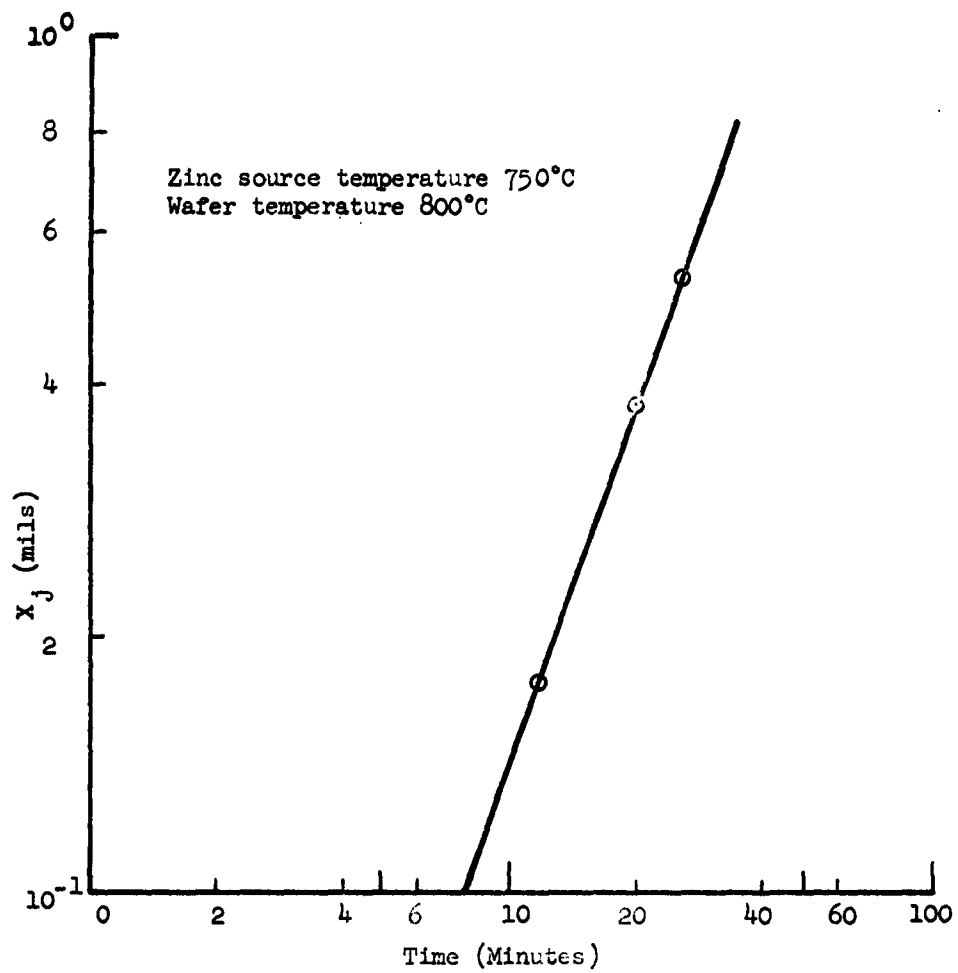


FIGURE 3 JUNCTION DEPTH  $X_j$ , AS A FUNCTION OF DIFFUSION TIME FOR ZINC INTO N-TYPE GaAs ( $n \approx 4 \times 10^{16}$  DONORS/cc)



$1.5 \times 10^{17}/\text{cm}$  and  $3 \times 10^{15}/\text{cm}$  by measuring the electron mobility and carrier concentration before and after a heat treatment which simulated the diffusion conditions normally used, until recently. The sample wafers were cleaned in reagent grade chemicals and sealed with a small amount of arsenic in an evacuated Vitreosil ampoule. They were then heated at  $1000^\circ\text{C}$  for three minutes in the glo-bar furnace normally used for diffusion. The data is summarized in Figures 4, 5 and 6. Figure 4 shows the normalized net carrier concentration change versus starting concentration for six samples measured. The average decrease in net donor concentration was about  $4 \times 10^{15}/\text{cc}$ . However, the electron Hall mobility remained constant, (Figure 5). The observed change in crystal resistivity (Figure 6) is, therefore, the result of the decrease in net carrier concentration only.

One technique which has been suggested to minimize the introduction of acceptors through the indiffusion of contaminants is the use of a radiant heat furnace for diffusion. (Ref.1)

In such a furnace the crystal can be maintained at a higher temperature than the quartz ampoule which is nearly transparent to radiant energy in the near infrared region of the spectrum. As a result, contamination from the quartz may be minimized. This technique will be investigated as a means of reducing the contaminants during diffusion.

### 3. Ohmic Contacts

A simple method has been devised to evaluate the contact resistance

---

(Ref.1) T.S. Kinsel and T.E. Seidel, "Heat Treatment of n-type GaAs by Radiant Energy", J.A.P. Feb., 1962.

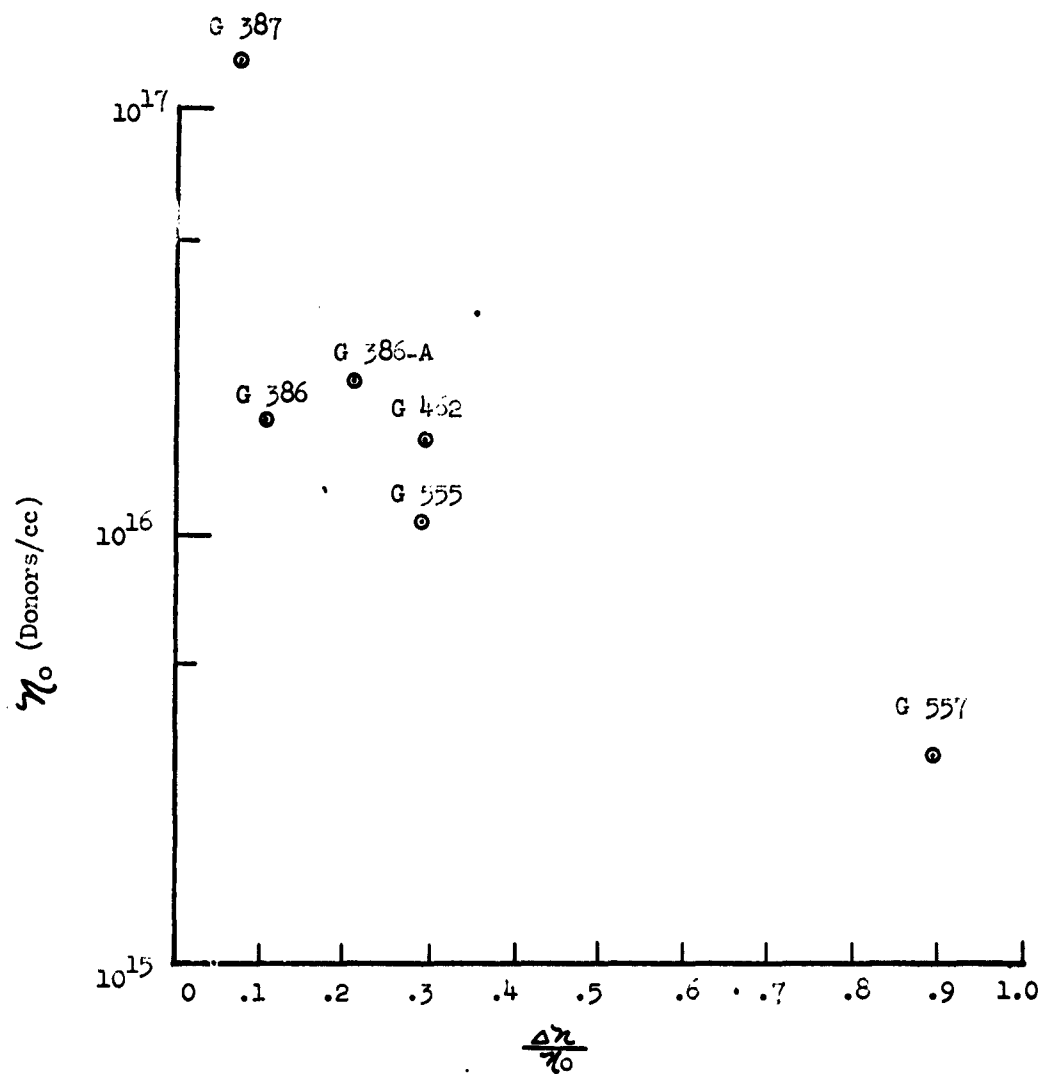


FIGURE 4 NORMALIZED NET CARRIER CONCENTRATION CHANGE vs. STARTING CONCENTRATIONS AFTER 3 MIN AT 1000°C FOR SEVERAL N-TYPE GaAs CRYSTALS

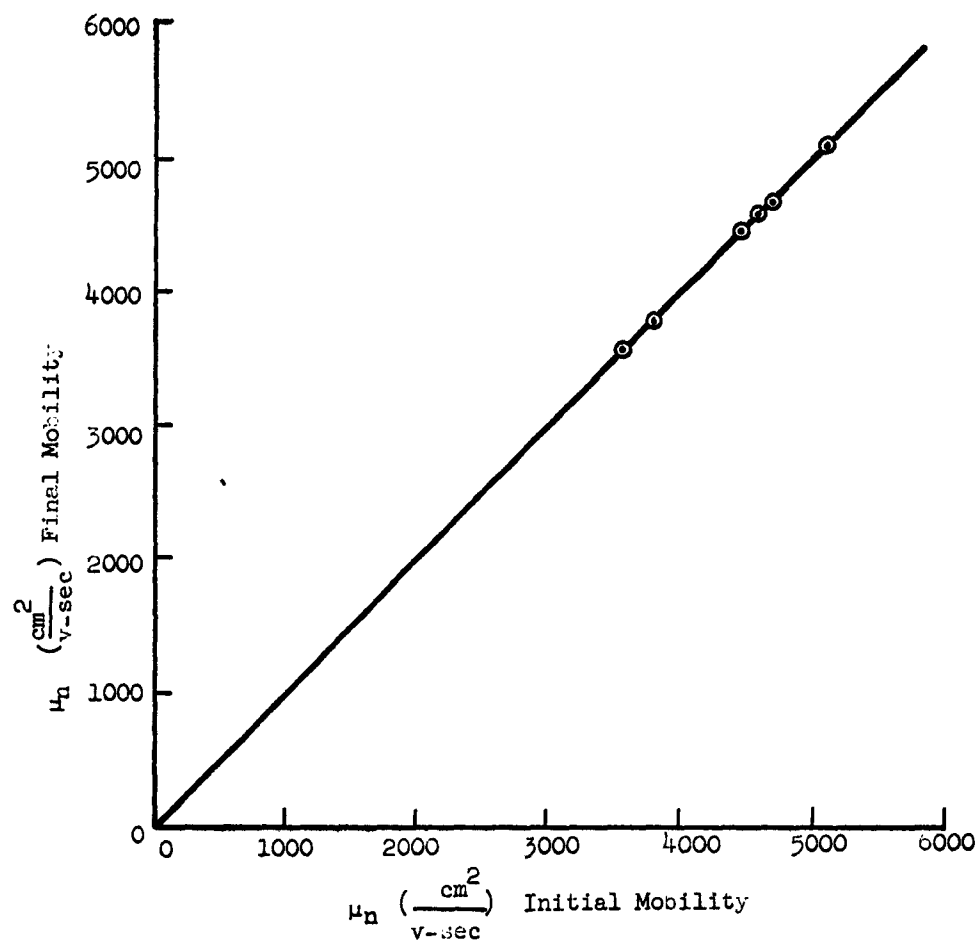


FIGURE 5 ELECTRON MOBILITY BEFORE AND AFTER HEAT TREATMENT  
(3 MIN AT 1000°C) FOR SIX N-TYPE GaAs SAMPLES

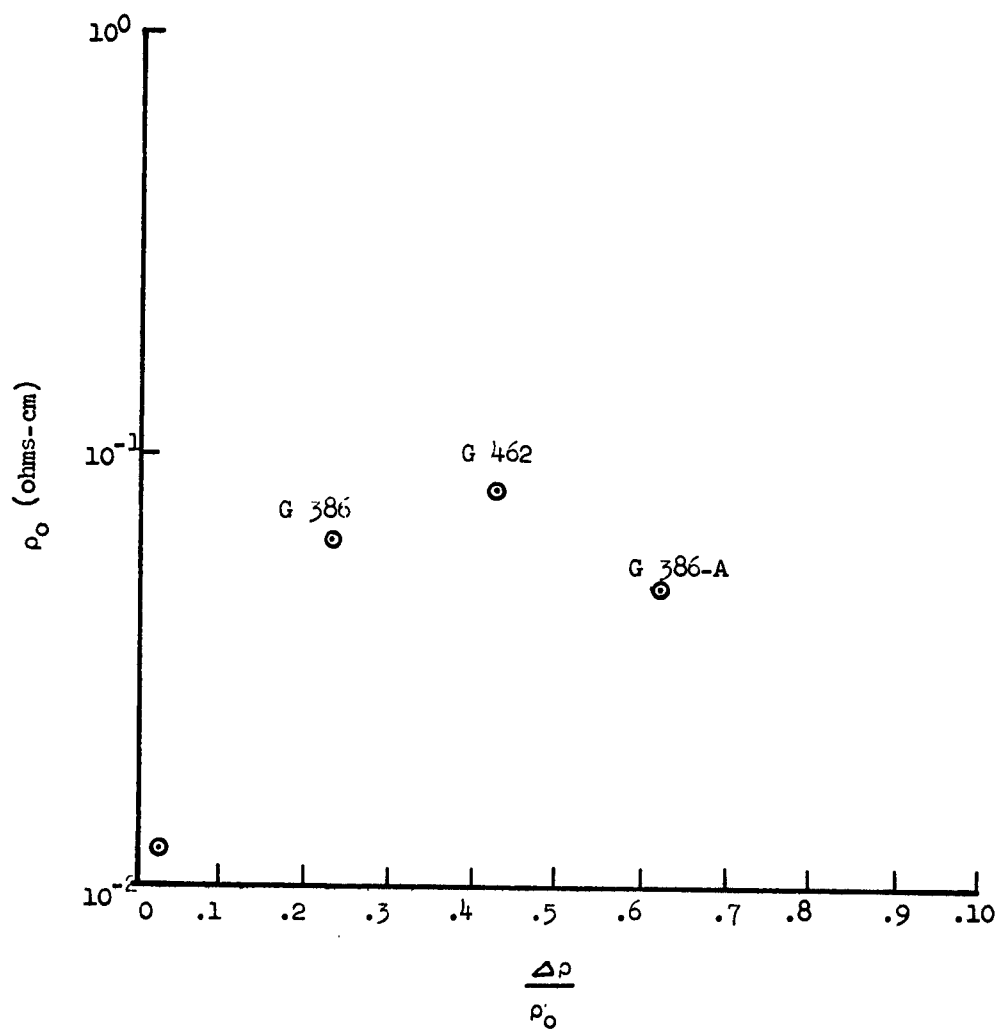


FIGURE 6 NORMALIZED RESISTIVITY CHANGE,  $\frac{\Delta \rho}{\rho_0}$ , vs. STARTING RESISTIVITY,  $\rho_0$ , FOR SEVERAL N-TYPE GaAs CRYSTALS DIFFUSED FOR 3 MINUTES AT 1000°C

of various alloys on gallium arsenide. A material for evaluation is alloyed into the gallium arsenide crystal in small inline areas across the chip, (Figure 7a). Two current probes and two separate voltage probes are connected to adjacent contact areas, (Figure 7b). A known current,  $I_1$ , is passed through the current probes and the voltage drop,  $V_1$ , is measured through the voltage probes. Figure 7d shows the equivalent circuit for the set-up.  $V_1 = I_1 (R_1 + R_s + R_2)$  where  $R_1$  and  $R_2$  are contact resistances and  $R_s$  the resistance of the gallium arsenide between the contact areas.

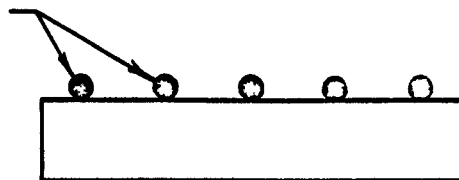
One of the current probes is then moved to another adjacent contact area and a known current  $I_2$  is passed through the current probes (Figure 7c). A voltage drop,  $V_2$ , is measured. From Figure 7e,  $V_2 = I_2 (R_1 + R_s)$ . If  $I_1 = I_2$ , then  $V_1 - V_2 = I_1 R_2$  and  $R_2$  can be determined.

The accuracy of the method is enhanced by using a relatively narrow crystal chip and small contact areas to minimize current spreading. The evaluation of various alloys is in progress.

#### 4. Epitaxial Diodes

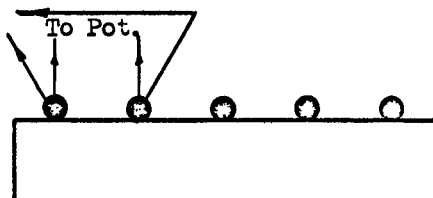
Two epitaxial wafers having grown  $p^+$  regions were evaluated. Such structures are of interest since p-type diffusion is eliminated, thus, reducing the possibility for introduction of contaminants into the crystal. The results are of interest, since the voltage breakdown characteristics of the diodes fabricated from these wafers were unusually uniform. Some of the typical device characteristics are listed in Table I. A85

Alloyed metallic contacts



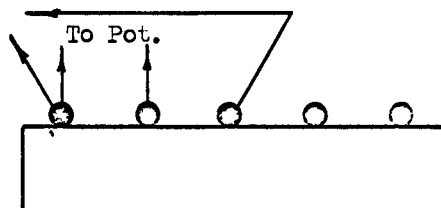
a. Crystal and Contacts

To Current Source

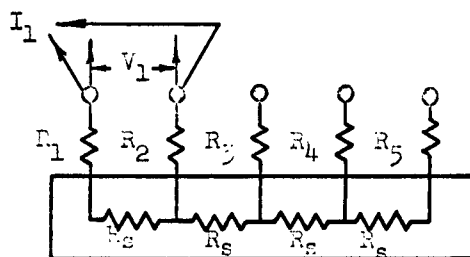


b. First Measurement

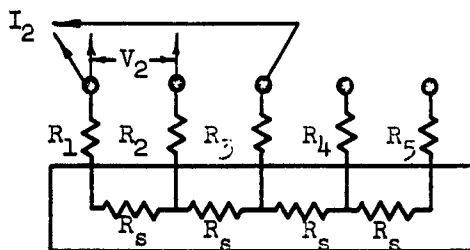
To Current Source



c. Second Measurement



d. Equivalent Circuit



e. Equivalent Circuit

FIGURE 7 CONTACT RESISTANCE DETERMINATION.

yielded diodes with exceptionally high breakdown voltages.

The computed junction impurity gradient calculated from capacitance per unit area data for wafer A85 is  $1.2 \times 10^{20}$  excess donors/cm<sup>4</sup>. From earlier data for non-epitaxial diodes, (Figure 8)<sup>(2)</sup> the observed breakdown voltage should be 90 volts, which agrees with the present results. Similarly for A84, the computed gradient is  $4 \times 10^{21}$  excess donors/cm<sup>4</sup>. The observed and expected breakdown voltage are again in agreement. The cutoff frequencies of these diodes are not higher than those achieved with non-epitaxial material. One possible reason may be the higher contact resistance of the connection to the p side of these pellets, the carrier concentration at the surface being lower than the ones normally achieved with diffused junctions. Furthermore, the n regions of these diodes are not substantially lower than the base of the "well" units fabricated from melt-grown gallium arsenide.

Diodes were also fabricated with diffused junctions on a number of nn<sup>+</sup> wafers. The best devices were fabricated on slice A75 having an exceptionally thin n-type epitaxial layer (0.15 mils) and a junction depth of 0.128 mils. The n-type layer carrier concentration was estimated to be approximately  $3 \times 10^{16}$ /cc. Three of these devices were submitted in fulfillment of Phase II of the contract (Table II).

---

(2) H.Kressel and A.Blicher, "Avalanche Breakdown in Graded Gallium Arsenide P-N Junctions" to be Published in J.A.P.

TABLE I  
CHARACTERISTIC OF GROWN P<sup>+</sup> NN<sup>+</sup> DIODES

Epitaxial Wafer Characteristics

Wafer No. A84

$$n = 3.45 \times 10^{16}, p^+ = 1.42 \times 10^{19}, n^+ = 5.7 \times 10^{18}$$

Thickness of n-region: 0.228 mils

Thickness of p<sup>+</sup> region: 0.37 mils

Wafer No. A85

$$n = 6.55 \times 10^{16}/\text{cc}, p^+ = 5 \times 10^{18}/\text{cc}, n^+ = 5 \times 10^{18}/\text{cc}$$

Thickness of n-region: 0.266 mils

Thickness of p<sup>+</sup> region: 0.32 mils

Diode No.	C <sub>jo</sub> (pf)	V <sub>B</sub> (volts)	f <sub>c-6</sub> (kmc/s) <sup>+</sup>
A84-6	.246	50.0	56
A84-8	.596	50.0	64
A84-4	.641	49.0	110
A84-7	.777	50.0	150
A85-14	.553	100.0	22
A85-13	.666	100.0	35
A85-8	.629	100.0	41

+ Measured at 10 kmc/sec



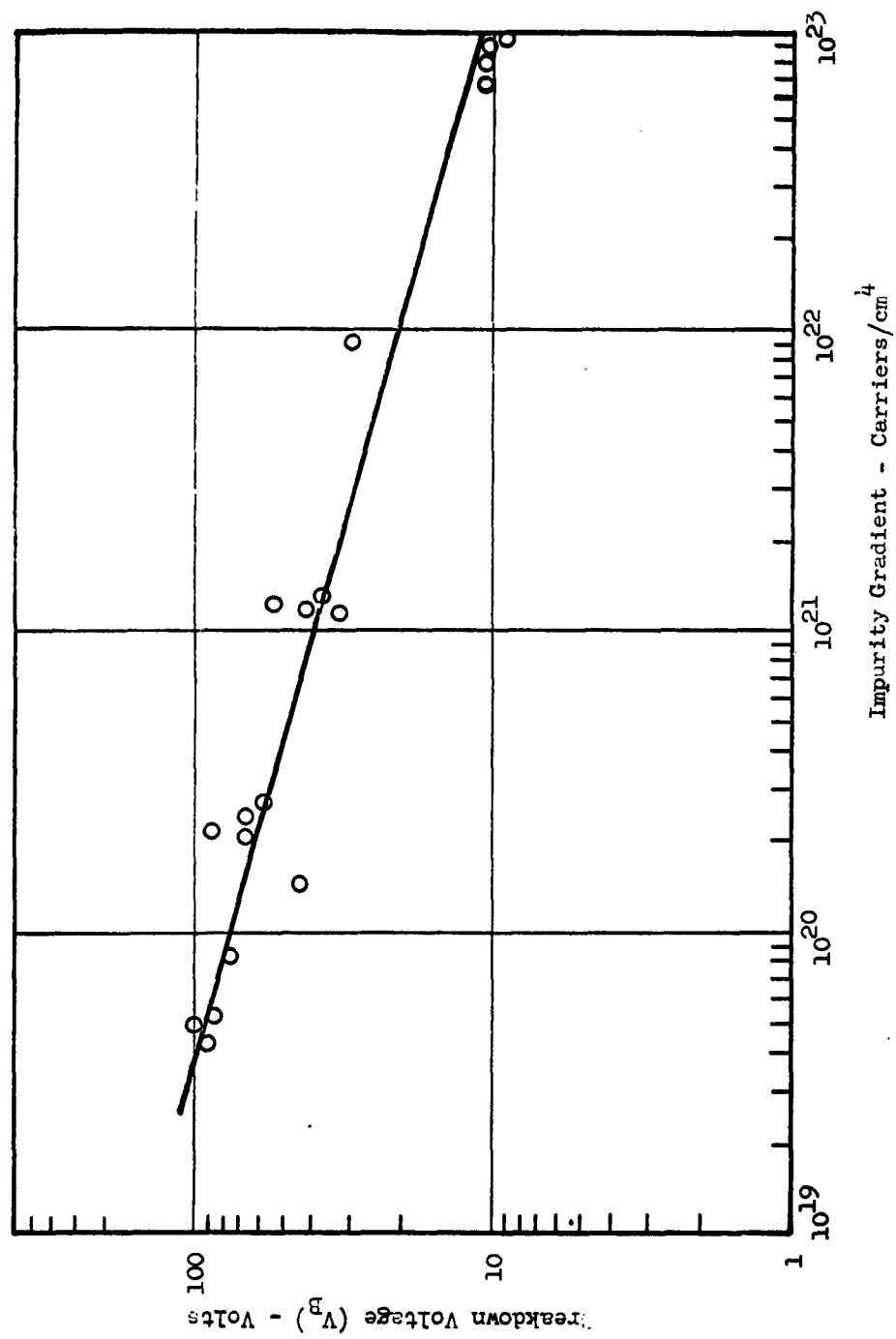


FIGURE 8 BREAKDOWN VOLTAGE AS A FUNCTION OF IMPURITY GRADIENT FOR PN GaAs JUNCTIONS

TABLE II

## DATA FOR VARACTOR DIODE - DEVICE B

Diode No.	$V_{BD}$ (volts)	$C_{j0}$ (pf)	$C_{j-2}$ (pf)	$C_{j \text{ min.}}$ (pf)	$Q$ (0-2V)	$f_{co-2}$ kmc	$f_{co \text{ max}}$ kmc
A795-5	33	.575	.388	.171	4.1	126	285
A796-24	32	.414	.293	.148	4.5	153	304
A801-19	44	.748	.512	.197	3.8	120	314
A816-1	33	.552	.381	.183	4.2	138	286
A823-6	30	.402	.288	.154	4.0	140	256
A921-10	28	.469	.330	.168	4.0	134	264
A45-3	38	.416	.302	.158	4.4	160	306
A75-10 <sup>+</sup>	47	.512	.351	.195	6.9	220	396
A75-2 <sup>+</sup>	20	.578	.391	.278	8.8	270	380
A75-15 <sup>+</sup>	30	.579	.374	.223	5.9	168	270

+ Epitaxial Unit

C. Final Results For Phase II

Table II lists the characteristics of the best devices fabricated during Phase II of the contract. These devices were submitted to the Contracting Agency on February 28, 1963. These diodes meet the breakdown voltage junction capacitance and cutoff frequency goals set forth in the Second Quarterly Report. The cutoff frequency was measured using the technique described in the First Quarterly Report.

### III. CONCLUSIONS

Improvements in process technology have made possible the fabrication of devices from melt grown GaAs with base widths of the order of 0.5 mils. High Q diodes have been fabricated with breakdown voltages in excess of 30 volts. A serious problem encountered in the fabrication of high breakdown diodes is the uncontrolled introduction during diffusion of p-type impurities which decreased the net carrier concentration of the material. This problem will be further investigated. Grown  $p^+ - n - n^+$  diodes appear promising if the  $p^+$  region is sufficiently doped. Diodes with breakdown voltages in excess of 100 volts have been made from such material.

## PART II

### I. PROGRAM FOR NEXT PERIOD

1. Improve cut-off frequency by reducing ohmic contact resistances.
2. Continue process developments for obtaining high cutoff frequency diode with breakdown voltages in excess of 30 volts.
3. Continue investigation of heat treatment effects on GaAs crystal, including epitaxially grown layers.